International Immunology, Vol. 21, No. 11, pp. 1277–1289
doi:10.1093/intimm/dxp094

Naive CD4 T cells from aged mice show enhanced death upon primary activation

Hamid Mattoo[1], Matthew Faulkner[2,*], Usha Kandpal[1,*], Rituparna Das[1], Virginia Lewis[2], Anna George[1,†], Satyajit Rath[1,†], Jeannine M. Durdik[2,†] and **Vineeta Bal[1,†]**

[1]National Institute of Immunology, Aruna Asaf Ali, Road, New Delhi 110067, India
[2]Department of Biological Sciences, University of Arkansas, Fayetteville, AR 72701, USA

Keywords: apoptosis, central memory, autophagy

Abstract

Poor T cell immunity is one of the many defects seen in elderly humans and aged (Ad) mice. We report that naive CD4 T cells from aged mice (ANCD4 cells) showed greater apoptosis upon primary activation than those from young (Yg) mice, with loss of mitochondrial membrane potential, poor activation of Rel family transcription factors and increased DNA damage. Their ability to enhance glycolysis, produce lactate and induce autophagy following activation was also compromised. ANCD4 cells remained susceptible to death beyond first cell division. Activated ANCD4 cells also showed poor transition to a 'central memory' (CM) CD44^{high}, CD62L^{high} phenotype *in vitro*. This correlated with low proportions of CM cells in Ad mice *in vivo*. Functionally, too, IFN-gamma responses recalled from T cells of immunized Ad mice, poor to begin with, worsened with time as compared with Yg mice. Thus, ANCD4 cells handle activation-associated stress very poorly due to multiple defects, possibly contributing to poor formation of long-lasting memory.

Introduction

Profound alterations in humoural and cellular immune responses are a hallmark of ageing, and understanding the mechanisms involved is key to the success of future vaccination strategies. Poor T cell function in the aged (Ad) leads to suboptimal antibody, CTL and cytokine responses to immunization (1–4). The total number of T cells with a memory phenotype increases with age (5), and the proportion of naive cells decreases. Further, recall responses generated to vaccines administered in the elderly humans are not long lasting (6), compounding the complexity. Additionally, in Ad animals, there is poor production of effectors from naive CD4 T cells, reversible in part or completely by IL-2 (7), possibly due to the ageing of individual T cells (8,9).

While non-T cell factors can contribute to poor naive T cell activation in the Ad (10,11), T cell-autonomous defects are prominent. Reported deficiencies in the TCR signalling pathway include early events such as calcium mobilization, NF-κB and NF-AT translocation (12), poor formation of the immunological synapse and poor recruitment of signalling intermediates to the synapse (13). Many of these defects contribute to a lack of production of IL-2, and exogenous IL-2 is shown to reduce the differences between young (Yg) and Ad T cells with reference to their activation-driven developmental progression (14). Ad naive T cells are suggested to be anergic (15), and their defective response could lead to either reduced clonal burst size or increased apoptotic death.

The susceptibility of the T cells from aged mice (aged T cells) to apoptosis is controversial. There is some evidence that activated aged T cells are less susceptible to Fas–FasL mediated death (16). On the other hand, in Ad humans naive, CM and effector memory (EM) cells are reported to be more susceptible to both Fas-mediated and tumor necrosis factor α-mediated apoptosis (17,18). Enhanced Bcl-2 expression in CD8 T cells from the aged is reported to contribute to their longer survival and reduced turnover (19). Cell death triggered by reactive oxygen species may (20) or may not (21) be increased in Ad T cells.

While it is generally accepted that naive aged T cells show defective activation (9), most of the studies concerned have used TCR-transgenic naive T cells either by themselves or in adoptive non-transgenic hosts (9,22,23). On this background, we have focussed our study on phenotypically naive polyclonal CD4 T cells from normal Ad mice. We report here that naive CD4 T cells from aged mice (ANCD4 cells) show an increased tendency to die during primary activation, in association with a poor metabolic response to activation,

*These authors have contributed equally; †These authors have contributed equally.

Correspondence to: V. Bal; E-mail: vineeta@nii.res.in

Received 10 April 2009, *accepted* 24 August 2009

Transmitting editor: M. Feldmann

Advance Access publication 11 September 2009

poor ability to repair DNA and a compromised autophagic process. We also show that this cell attrition during primary activation is associated with poor generation of CD4 T cells of the CM phenotype, both *in vitro* and *in vivo*.

Methods

Mice

C57BL/6 and B6.lpr mice obtained from the Jackson Laboratory (Bar Harbour, ME, USA) and bred at the small animal facilities of either the National Institute of Immunology, New Delhi, India, or the University of Arkansas, Fayetteville, AR, USA, were used. All Yg mice were used at 2–3 months of age, while all Ad mice were between 18 and 20 months of age at the initiation of the experimental procedure. Ad mice were either maintained for ageing in-house in the two animal facilities above or obtained from the Ad mouse colony of the National Institute on Ageing, National Institutes of Health (NIH), Bethesda, MD, USA. Mice deficient in c-Rel bred to the C57BL/6 background were the kind gift of H. C. Liou, Cornell University, New York, NY, USA, and Ranjan Sen, National Institute on Ageing, Baltimore, MD, USA. All mice were maintained and used according to the guidelines of the respective institutional animal ethics, care and use committees.

Immunizations

Mice were immunized subcutaneously in the footpad with 100 μg maleylated ovalbumin (mOA) in CFA (Difco, Detroit, MI, USA). Ovalbumin was maleylated as described previously (24). Seven, 28 and 45 days later, draining popliteal and inguinal lymph nodes were isolated and single-cell suspensions made for assays described below.

Reagents

RPMI-1640 (Biological Industries, Kibbutz Beit Haemek, Israel) appropriately supplemented with antibiotics and FCS was used throughout in cultures. Reagents used for staining were as follows: various fluorophores or biotin coupled with mAbs to CD4, CD8, CD44, CD62L and CD69 (e-Biosciences, San Diego, CA, USA, and BD Biosciences, San Diego, CA, USA). For biotinylated mAbs, streptavidin coupled to various fluorophores as indicated was used as a secondary reagent. Fluorescein or PE-labelled annexin V (BD Biosciences) was used to score apoptotic death with protocols recommended by the manufacturers. Rabbit polyclonal antibody to microtubule-associated protein light chain-3 (LC3; Santa Cruz Biotechnology, Santa Cruz, CA, USA) was used along with goat–anti-rabbit antibody coupled to Alexa fluor 488 (Invitrogen, Carlsbad, CA, USA) as the secondary reagent.

Purification of T cells using magnetic cell separation

Pooled splenic cells from 2–3 mice were stained with a biotin-conjugated cocktail of anti-CD44, anti-B220, anti-CD11b and anti-CD8 mAbs to purify naive CD4 cells. For purification of CD4+ EM ($CD44^+CD62L^-$) cells, anti-CD62L mAb replaced anti-CD44 mAb in the above cocktail. Using streptavidin-coupled beads, cell purification was done by negative selection on magnetic columns according to manufacturer's protocols (Miltenyi Biotech, Bergisch Gladbach, Germany). Purity of the separated populations was consistently >90% (see Supplementary Data, Fig. S1, available at *International Immunology* Online). At this point >98% of the cells were viable as checked by Trypan blue exclusion and >95% by annexin V.

In vitro T cell stimulation assays

ANCD4 cells and naive CD4 cells from young mice (YNCD4 cells) or *ex vivo* purified CD4+ EM cells from Yg and Ad mice were stimulated *in vitro* with plate-coated anti-CD3 and anti-CD28 mAbs (1 and 5 μg ml^{-1} respectively; BD Biosciences) or bead-coated anti-CD3 and anti-CD28 mAbs (Dynal via Invitrogen; used at a 1 : 1 cells : beads ratio] and were compared with unstimulated cells. Under these activating conditions, the first division of ANCD4 and YNCD4 cells was observed to take place after 36 h (data not shown). Where indicated, 3-methyl adenine (3-MA; Sigma Aldrich, Bangalore, India) was added at a final concentration of 1 mM.

T cell blasts were prepared as described earlier (25). Briefly, ANCD4 and YNCD4 cells were stimulated with anti-CD3 and anti-CD28 mAbs for 48 h, and cells were cultured in the presence of 5 U ml^{-1} of IL-2 for a further 48 h. At the end of 96 h, viable cells were obtained by density-gradient centrifugation. These 96-h T cell blasts were subjected to further experiments.

For measuring proliferation of *ex vivo* purified EM cells or 96-h T cell blasts, 1×10^5 T cells were cultured in anti-CD3-coated 96-well plates and were pulsed at 48 h for measurement of [^{3}H]thymidine incorporation. Data are expressed as mean ± SEM of triplicate cultures.

For antigen-specific recall assays, draining lymph node cells were stimulated with 100 μg ml^{-1} of mOA. Levels of secreted IFN-gamma were measured from culture supernatants collected at 48 h by ELISA, essentially following manufacturer's recommendations (BD Biosciences). Standards were run in parallel to enable calculation of concentrations of IFN-gamma.

Flow cytometry

For flow cytometry, cells were stained with primary and secondary antibodies as appropriate on ice, washed and analysed immediately. For cell cycle analysis, cells were harvested, fixed and permeabilized by 70% ethanol and propidium iodide (PI) was added at a final concentration of 10 μg ml^{-1}. For scoring the cells undergoing loss of mitochondrial potential, cells were stained with 3,3′-dihexyloxacarbocyanine iodide ($DiOC_6$; Molecular Probes, Invitrogen) in serum-free medium and PI was added to a final concentration of 1 μg ml^{-1}. Cells were analysed immediately. Stained samples were run either on FACSort, LSR I or FACSaria flow cytometers (Becton and Dickinson, San Jose, CA, USA), and data were analysed using FlowJo software (Tree Star, San Carlos, CA, USA).

Comet assay

ANCD4 and YNCD4 cells were activated for 12 or 24 h and harvested, and dead cells were removed by density-gradient centrifugation so that viability of the cells assayed was ~99% by Trypan blue exclusion test before assay. The cell

suspension was then mixed with low-melting agarose and poured on a slide. The relative proportions of DNA with breaks in individual cells were measured following the alkaline comet assay procedure (26). Alternatively, ANCD4 and YNCD4 were exposed to 3 Gy gamma-radiation using Co^{60} as a source and the extent of damaged DNA was scored as above after 12 h. Pictures were taken under a fluorescence microscope (Olympus America Inc., Center Valley, PA, USA) and between 30 and 60 cells were analysed per sample by CometScore software (TriTek Corp., Virginia, VA, USA) (26).

Confocal microscopy and quantitation

Stimulated or unstimulated ANCD4 and YNCD4 cells were harvested at indicated times, fixed and permeabilized using 0.5% saponin and 4% paraformaldehyde (both from Sigma Aldrich) as a modification of a published method (27). Cells were stained with rabbit–anti-LC3 antibody followed by goat–anti-rabbit F[ab′]2-Alexa fluor 488. Cells were also stained with anti-CD4 and DAPI to visualize the cell surface and nucleus, respectively. Cells were analysed under a Leica TCS SP2 laser confocal microscope (Leica Microsystems, Wetzlar, Germany). Quantification was done with stacked images using Leica Confocal Software.

Western blot analysis

ANCD4 and YNCD4 cells were stimulated, harvested at different time intervals and nuclear and cytosolic fractions were prepared using NE-PER kit (Pierce Biotechnology, Rockford, IL, USA). After electrophoresis and sample transfer, nitrocellulose membranes (Advanced Microdevices, Ambala, India) were probed with polyclonal antibodies to actin, c-Rel or p65 (Santa Cruz Biotechnology). Bands were visualized by the enhanced chemiluminescence method following the manufacturer's recommendations (Amersham Biosciences, Little Chalfont, UK). Image J software (NIH, Bethesda, MD, USA) was used for densitometry.

Lactate estimation

ANCD4 and YNCD4 cells were activated and at various time points lactate levels were estimated following the procedure recommended by the manufacturer (Eton Biosciences, San Diego, CA, USA). A standard was run in parallel to calculate actual values.

Statistical analysis

Multiple independent experiments with independent sample sets were done for all data shown. Data are shown as data point scatter and mean for data analysed by the Mann–Whitney *U*-test and as mean ± SEM for data analysed by the unpaired two-tailed Student's *t*-test. Observations were considered statistically significant if P value was <0.05.

Results

ANCD4 cells are more prone to death upon primary activation than YNCD4 cells

Purified splenic YNCD4 or ANCD4 cells were put in culture with or without plate-coated anti-CD3 and anti-CD28, and viable cell numbers were estimated at various time points using Trypan blue exclusion. As early as 12 h post-activation, the recovery of viable cells from stimulated cultures of Ad cells was poorer than that from Yg cell cultures (Fig. 1A) and this trend continued at 24 h (Fig. 1B). In contrast, unstimulated ANCD4 cells survived as well or better than YNCD4 cells (data not shown). The cell death involved is apoptotic as demonstrated by using annexin V to stain cells from these cultures at various times. Both at 12 and 24 h of activation, ANCD4 cells showed more apoptotic death than YNCD4 cells (Fig. 1C, right panels), while resting ANCD4 cells survived better than YNCD4 cells did at the same time points (Fig. 1C, left panels). Data from multiple such experiments scoring apoptotic death at 12 or 24 h showed significantly greater apoptosis in ANCD4 cells upon activation, but no difference in the absence of activation (Fig. 1D).

In order to determine the role of mitochondrial death pathways in this apoptotic cell death, cells were labelled with the mitochondrial dye $DiOC_6$ and co-stained with PI after various times in culture. At 12 h post-activation, activated ANCD4 cells showed a greater frequency of cells with low $DiOC_6$-staining intensity without PI staining (Fig. 1E), as shown in data from multiple independent experiments (Fig. 1F), indicating early mitochondrial membrane potential loss and suggesting that mitochondrial damage was occurring prior to loss of cell viability. ANCD4 cells also showed greater death as scored by PI staining than YNCD4 cells at both 12 and 24 h post-activation (Fig. 1E–H).

Higher proportion of subdiploidy and defective DNA repair in ANCD4 cells post-activation

We used PI staining of permeabilized cells to follow the progression of ANCD4 cells through cell cycle and to estimate the proportions of subdiploid cells upon activation. At 20 h of culture, the frequency of subdiploid apoptotic cells was higher in stimulated ANCD4 cells (Fig. 2A and B) than in YNCD4 cells in multiple independent experiments. The data suggested that cells were undergoing death before DNA replication is completed. Since defective DNA repair during the cell cycle can contribute to apoptosis (28), we also evaluated the extent of DNA damage in naive CD4 cells at 12 and 24 h post-activation using the alkaline comet assay (26). The data showed that at these early time points, the damaged DNA content in comet tails, using tail moment as a parameter, was greater in stimulated ANCD4 cells as compared with YNCD4 cells (Fig. 2C). In order to ensure that the damaged DNA detected in these assays was not simply from dead cells, cells were purified post-activation by density-gradient centrifugation before comet assays were set up. Comet tails were larger in ANCD4 cells than in YNCD4 cells (see Supplementary Fig. S2, available at *International Immunology* Online). Cells receiving 3 Gy radiation were used as a positive control for this assay and we found that ANCD4 cells exposed to radiation damage showed higher tail moment at 12 h as compared with YNCD4 cells (Fig. 2D, see also Supplementary Data, Fig. S3, available at *International Immunology* Online).

In order to correlate DNA damage and T cell activation further, we looked at the susceptibility of activated ANCD4 cells to death following gamma-irradiation using flow cytometry. ANCD4 and YNCD4 cells that received 1-, 3- or 10-Gy

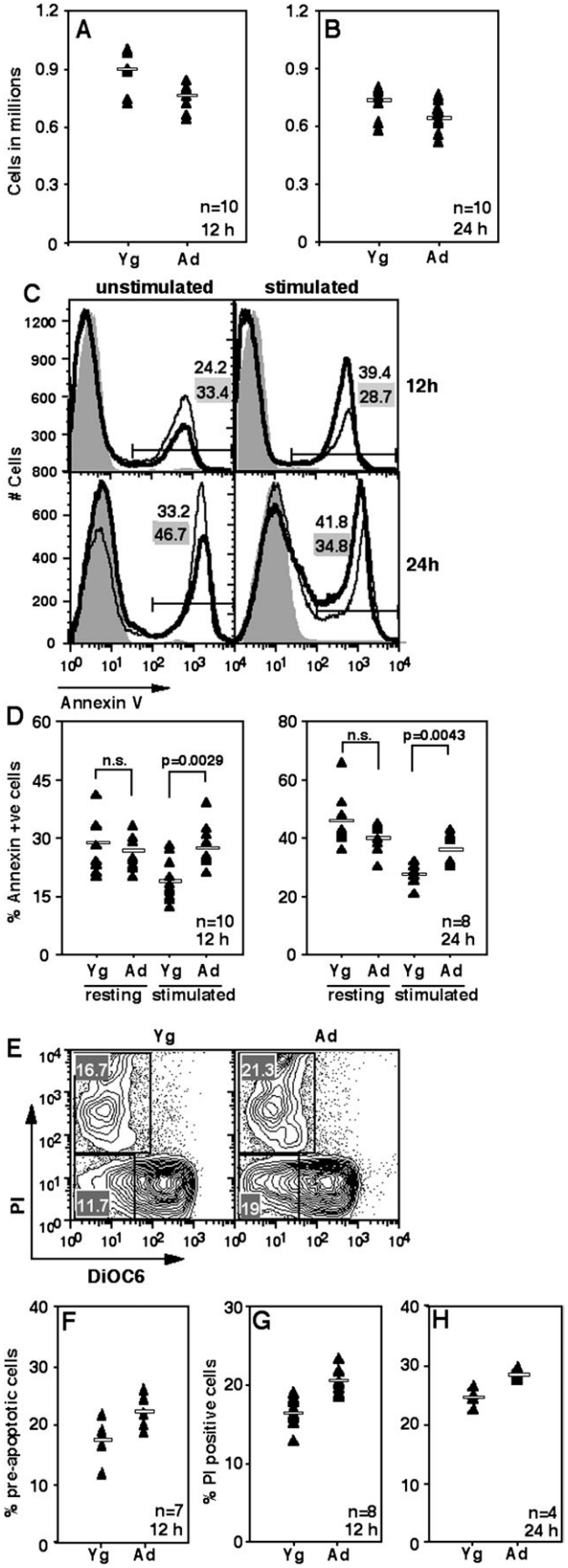

radiation doses were activated with anti-CD3 and anti-CD28 and cell death was measured 12 h later in activated cells showing CD69 induction. In cultures of non-irradiated cells, CD69-expressing activated ANCD4 cells died at higher frequency than YNCD4 cells (Fig. 2E). With increasing dose of radiation the proportion of cell death went up more rapidly in ANCD4 cells than in YNCD4 cells (Fig. 2E).

In the culture conditions used here, the first cell divisions were detectable by carboxyfluorescein succinimidyl ester (CFSE) labelling at ~36 h post-activation (data not shown). Thus, the above data indicate that the activation-associated cell death seen here occurs prior to any cell division.

Defective NF-κB induction in ANCD4 cells

T cell stimulation induces the activation of transcription factors of the Rel family, which are known to play a major role in regulating cellular commitment to apoptosis (29). There are previous reports that induction of Rel family members is poor in T cells from Ad animals (30,31). We confirmed these findings in the ANCD4 cells used here. Since prolonged induction of NF-κB is reported to be required for complete T cell activation and survival (32), we used the 30- to 90-min post-activation time points for the NF-κB assay, as has been used earlier (33). When activated naive CD4 T cells were examined for nuclear translocation of the Rel-family proteins, p65 and c-Rel, by western blot analysis, it was evident that, while there was no appreciable difference in cytosolic levels, nuclear translocation of both p65 and c-Rel was poor in Ad cells (Fig. 3A). Pooled data from multiple experiments showing p65/actin (Fig. 3B) and c-Rel/actin (Fig. 3C) ratios in nuclear extracts 60 min post-activation confirmed the finding. These data suggest a possible role for Rel-family transcription factors in controlling early death decisions during primary activation of naive CD4 T cells.

Metabolic defects in ANCD4 cells

A major consequence of T cell activation is an increase in metabolic demands, met by increased glucose uptake and

Fig. 1. Ad naive CD4 T cells die more on activation. (A and B) Trypan blue-negative cell counts in anti-CD3+anti-CD28-stimulated naive CD4 cells at 12 (A) or 24 h (B) of culture. (A) $P = 0.004$; (B): $P = 0.0087$ by Mann–Whitney test. Horizontal line in each panel depicts the mean value; *n* as indicated. (C) Proportions of annexin V-binding cells from unstimulated (left panels) and stimulated (right panels) NCD4 cell cultures at 12 (top panels) and 24 h (bottom panels).Thin line: Yg cells; thick line: Ad cells. Shaded histogram, negative control. Numbers with grey backgrounds show proportions of cells from YNCD4 cultures and those with white backgrounds from ANCD4 cultures. (D) Pooled data as in C from 8–10 experiments showing proportions of annexin V-binding cells from Yg and Ad mice in resting (unstimulated) and stimulated cultures at 12 (left panel) and 24 h (right panel). *P* values as shown by Mann–Whitney test; n.s. = not significant. Horizontal line in each panel depicts the mean value; *n* as indicated. (E) Staining profiles of $DiOC_6$- and PI-labelled YNCD4 (left panel) and ANCD4 (right panel) cells 12 h post-activation. Numbers in various quadrants indicate percentages. (F) Proportions of $DiOC_6^{low}$, PI^- pre-apoptotic cells from cultures 12 h post-activation. $P = 0.0102$ by Mann–Whitney test; *n* as indicated. Horizontal line depicts mean value. (G and H) Proportions of $DiOC_6^{low}$, PI^+ cells from stimulated cultures at 12 (G) and 24 h (H) post-activation. (G): $P = 0.0008$ and (H): $P = 0.05$ by Mann–Whitney test; *n* as indicated. Horizontal line depicts mean value.

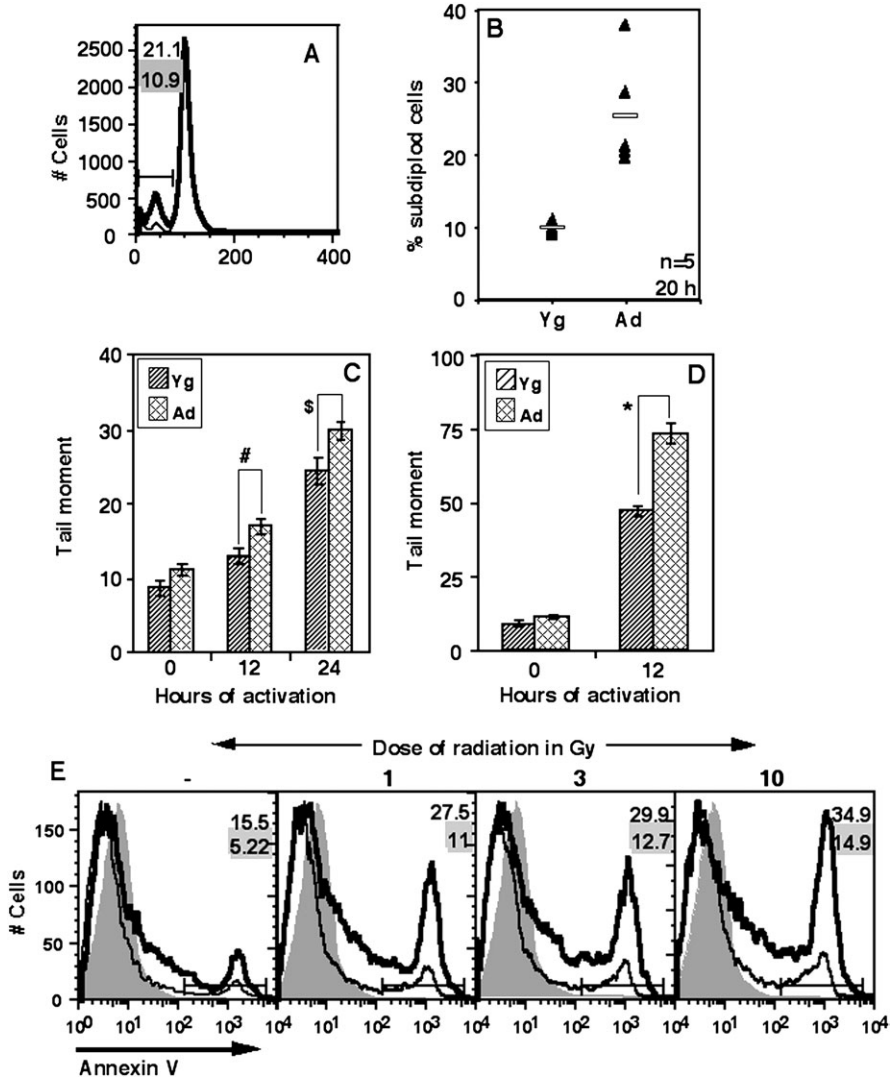

Fig. 2. Ad naive CD4 T cells show more subdiploidy and defective DNA repair post-activation. (A) A representative analysis of DNA content of stimulated YNCD4 and ANCD4 cells after 20 h in culture. Subdiploid population is marked in PI-stained cells. Numbers with grey background are for Yg cells, and those with white background for Ad cells. (B) Percentages of subdiploid cells from stimulated YNCD4 and ANCD4 cultures are shown. $P = 0.006$ by Mann–Whitney test; n as indicated. Horizontal line depicts mean value. (C and D) Comparison of ANCD4 and YNCD4 cells activated with anti-CD3+anti-CD28 (C) or irradiated (3 Gy) (D) and scored for tail moment over indicated period (mean ± SEM, $n = 30–60$ cells, $\#P = 0.0048$, $\$P = 0.0126$, $*P = 0.0000$ by Student's t-test). (E) ANCD4 and YNCD4 cells, irradiated with indicated doses or left unirradiated, were activated with anti-CD3+anti-CD28 and 12 h post-activation and stained with anti-CD69 and annexin V. Comparison of annexin V binding in gated CD69-expressing cells is shown. Thin line: Yg cells; thick line: Ad cells. Data are representative of two independent experiments. Numbers with grey background are for Yg cells, and those with white background for Ad cells.

anaerobic glycolysis, resulting in the production of pyruvate and lactate (27). We therefore looked at the levels of lactate produced by activated ANCD4 and YNCD4 cells. While background levels were comparable in the two groups, activated YNCD4 cells at 30 h had significantly higher lactate levels as compared with ANCD4 cells (Fig. 3D), indicating that ANCD4 cells were inefficient at using anaerobic glycolysis for meeting increased energy demands during activation.

Another modality that cells use to meet metabolic demands is autophagy, which can under such circumstances act as a survival mechanism (34). We therefore estimated the extent of induction of autophagy in ANCD4 and YNCD4 cells using confocal microscopic detection of LC3 fluorescence around autophagic vacuoles (see Supplementary Data, Fig. S4, available at *International Immunology* Online). By 12 h post-activation, the extent of LC3 fluorescence was much higher in YNCD4 cells as compared with ANCD4 cells (Fig. 3E). If autophagy is indeed involved in meeting the metabolic needs of activated T cells and maintaining their viability, a prediction would be that inhibition of autophagy during activation would enhance apoptosis in YNCD4 cells. We tested this using 3-MA to inhibit autophagy. In the presence of 3-MA, YNCD4 cells showed higher proportion of cell death at 24 h post-activation, while there was no effect on ANCD4 cell death (Fig. 3F), which show poor autophagy to start with. Pooled data from independent

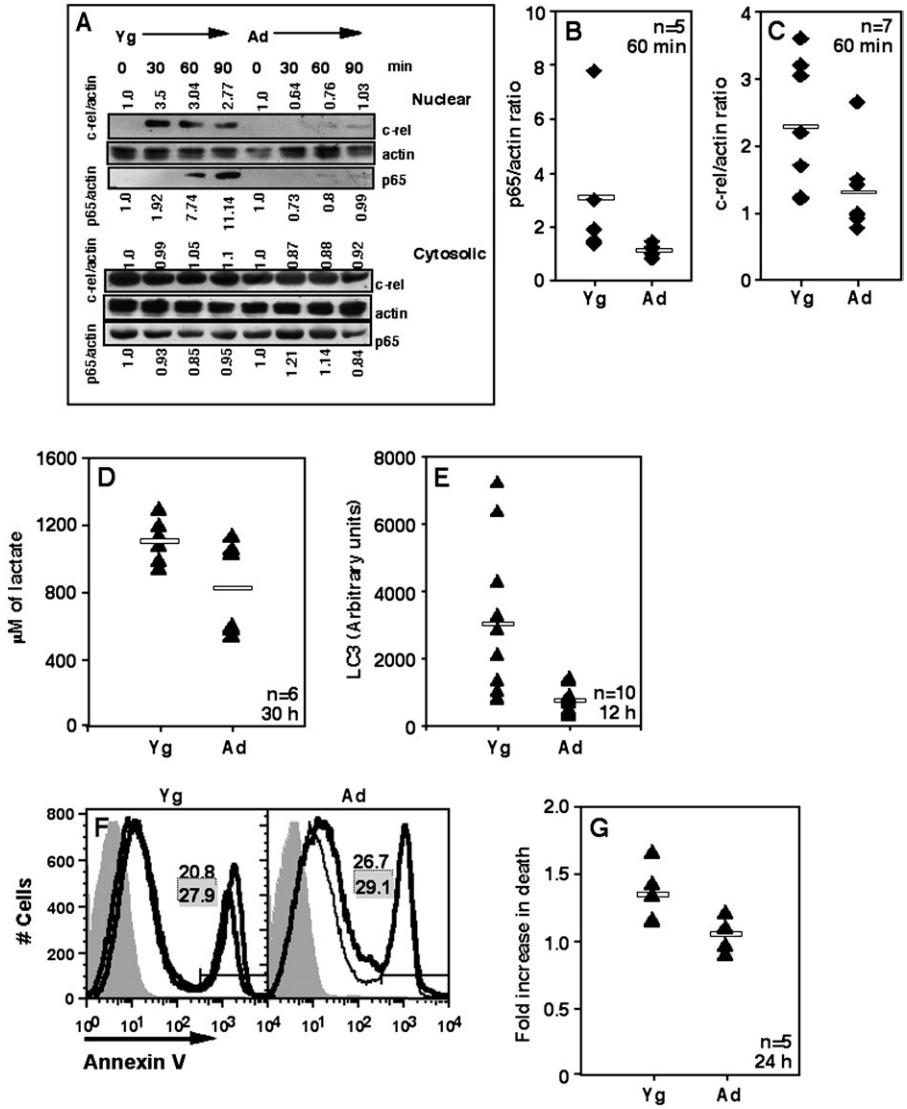

Fig. 3. ANCD4 cells show defects in NF-κB induction, metabolism and autophagy. (A) Western blot showing poor nuclear translocation of p65 and c-Rel in activated ANCD4 as compared with YNCD4 cells. Nuclear (top) and cytoplasmic (bottom) levels at various times post-activation as shown. Normalized ratios for p65/actin and c-Rel/actin shown below and above each cluster of western blots, respectively. Zero-hour ratio for each set designated as 1. Data are representative of five to seven independent experiments. (B and C) Fold enhancement in signal as p65/actin (B) and c-Rel/actin (C) ratios in the nuclear extracts of 60-min-activated ANCD4 and YNCD4 cells. (B): $P = 0.0107$ and (C): $P = 0.0207$ by Mann–Whitney test; n as indicated. Horizontal line depicts mean value. (D) Levels of lactate in cultures from ANCD4 and YNCD4 cells 30 h post-activation. $P = 0.0465$ by Mann–Whitney test; n as indicated. Values of lactate at 0 h: Yg 822.7 ± 31.44 and Ad 841.15 ± 48.62 µM (mean ± SEM). Horizontal line depicts mean value. (E) ANCD4 and YNCD4 cells were activated for 12 h and intensity of LC3 staining around autophagosomal vacuoles was estimated by quantitative fluorescence microscopy. $P = 0.0014$ by Mann–Whitney test; n as indicated. Intensity at 0 h: Yg 881.7 ± 184.7 and Ad 1132.49 ± 155.28 (mean ± SEM, $n = 10$). Horizontal line depicts mean value. (F) Annexin V staining of YNCD4 and ANCD4 cells stimulated for 24 h in the presence (thin line) or absence (thick line) of 1 mM 3-MA. Shaded histogram, negative control. Proportions in the absence (white background) or presence (grey background) of 3-MA shown as numbers in each panel. Data are representative of five independent experiments. (G) Fold increase in death in the presence of 3-MA 24 h post-activation. Data shown as % death in the presence of 3-MA/% death in the absence of 3-MA. $P = 0.0183$ by Mann–Whitney test; n as indicated.

experiments show a significant difference in fold enhancement in death in the presence of 3-MA in YNCD4 and ANCD4 cells (Fig. 3G).

ANCD4 cells continue to die more at later stages during in vitro activation

We next tested the possibility that successful transition through cell cycle would protect ANCD4 cells against the enhanced cell death seen during early stages of activation. Trypan blue-negative cell counts showed lower yields in activated ANCD4 cells at 48 and 60 h post-activation (data not shown). When cell cycle analysis was done on these cultures at 40 h by which time the first division had taken place, the pattern observed at 20 h was maintained, with ANCD4 cells from stimulated cultures showing significantly greater frequencies of apoptotic subdiploid cells in multiple

experiments (Fig. 4A and B). CD44 is an activation marker that is expressed at time points later than CD69 is and is stably maintained. Therefore, at 48 h post-activation, cultures activated as above were stained for CD44 and CD44^{high} cells were examined for apoptosis using annexin V. CD44^{high} cells from activated ANCD4 cultures showed increased death (Fig. 4C) that was statistically significant (Fig. 4D).

Since activated T cell populations do not synchronously enter cell cycle, and since aged T cells are likely to show different kinetics of activation-induced cell division *in vitro*, we specifically analysed death in dividing cells in comparable generations. CFSE-labelled YNCD4 and ANCD4 cells were stimulated *in vitro* as above, and 48 (Fig. 4E) or 60 h (Fig. 4I) post-activation, cells in successive generations were gated as shown (rightmost panels in Fig. 4E and I) for examination of annexin V binding. A representative profile of annexin V positivity in generation 0, 1 and 2 for 48 and 60 h, respectively, is shown (Fig. 4E and I). Data from multiple experiments for generations 0, 1 and 2 for 48 h (Fig. 4F–H) and 60 h (Fig. 4J–L) are shown. While Ad cells showed poor proliferation in response to stimulation as expected (data not shown), the difference in the susceptibility to death of ANCD4 and YNCD4 decreased with successive generations. Thus, by second generation at 48 h (Fig. 4H) and first and second generation at 60 h (Fig. 4K and L) the difference was not statistically significant, suggesting emergence of a relatively apoptosis-resistant population in the ANCD4 cells.

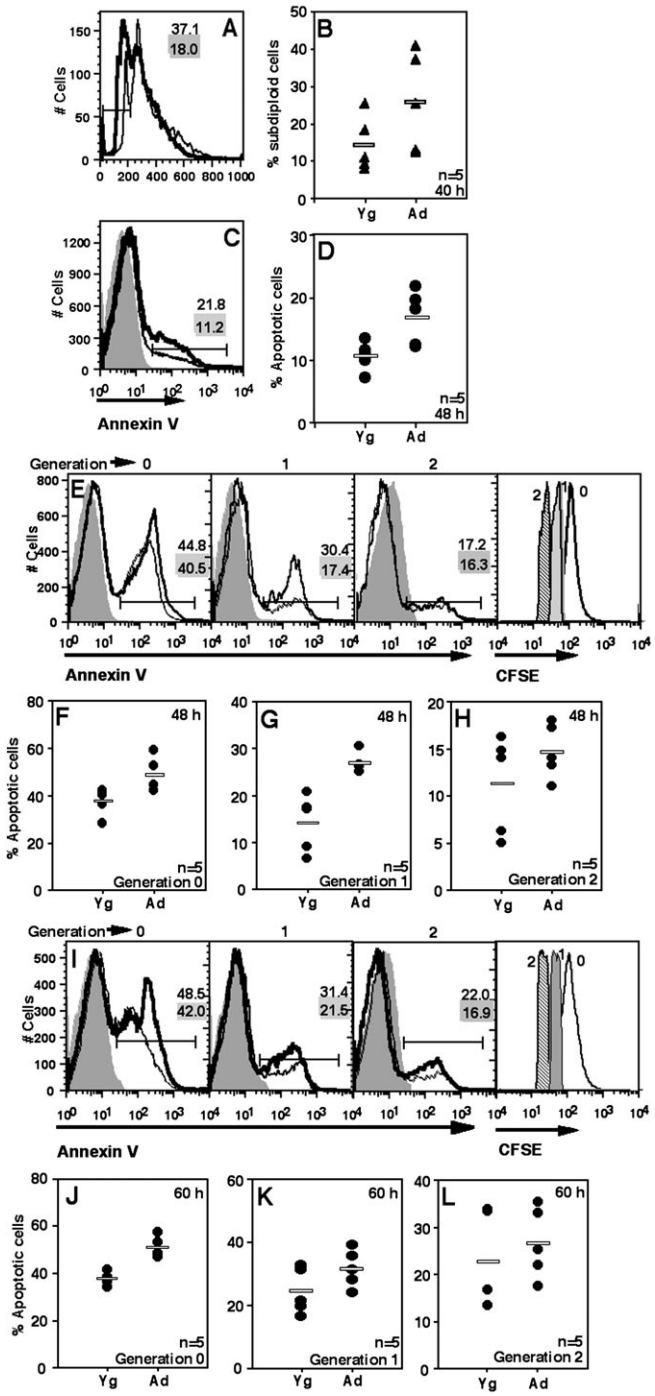

Fig. 4. ANCD4 cells continue to die at higher frequency for some successive generations. (A) A representative profile of ANCD4 and YNCD4 cells 40 h post-activation to show subdiploid cells using post-permeabilization PI staining. Numbers with grey background are for Yg cells; numbers with white background are for Ad cells. (B) Data from five independent experiments as in (A) above showing proportions of subdiploid cells from ANCD4 and YNCD4 cultures. P = 0.0475 by Mann–Whitney test. Horizontal line depicts mean value. (C) ANCD4 and YNCD4 cells were activated for 48 h and death scored in CD44^{high} cells by annexin V. Thin line: YNCD4; thick line: ANCD4. Numbers with grey background are for YNCD4; numbers with white background are for ANCD4. (D) Percentages of apoptotic cells from five independent experiments in CD44^{high} ANCD4 and YNCD4 cells at 48 h post-activation. P = 0.0183 by Mann–Whitney test. Horizontal line depicts mean value. (E–L) After activation for 48 (E, F, G, H) or 60 h (I, J, K, L), successive cell generations were gated in CFSE-labelled ANCD4 and YNCD4 cells, and the proportions of annexin V-positive cells in each cell generation estimated. Representative histograms are shown (E, I); thin line: YNCD4; thick line: ANCD4. Numbers with grey background are for YNCD4; numbers with white background are for ANCD4. Representative CFSE profiles of populations in generation 0, 1 and 2 are shown in the rightmost panels in (E) and (I). Proportions of apoptotic cells in generations 0, 1 and 2 at 48 (F, G, H) and 60 h (J, K, L) are shown. (F): P = 0.0107; (G): P = 0.006; (H): P = 0.2643; (J): P = 0.006 and (K): P = 0.0869; (L): P = 0.2 by Mann–Whitney test; n as indicated. Horizontal line depicts mean value.

T cell blasts generated in vitro and ex vivo EM cells from Ad and Yg mice show equivalent susceptibility to death.

Addition of exogenous IL-2 leads to substantial improvement in the proliferative response of Ad CD4 T cells to TCR-mediated stimulation, and the surviving T cell blasts undergo extensive proliferation by 96 h in such supplemented stimulation cultures. We next asked whether such T cell blasts of aged CD4 T cells still continued to show differential susceptibility to death. Therefore, we compared the susceptibility of 96-h T cell blasts generated by activation with anti-CD3 and anti-CD28 in the presence of IL-2 from YNCD4 or ANCD4 cells to death during secondary stimulation.

YNCD4 and ANCD4 T cell blasts were stimulated with titrating concentrations of soluble anti-CD3 and irradiated splenic antigen-presenting cells. Unlike freshly isolated naive CD4 cells, ANCD4 T cell blasts showed proliferative

responses equivalent to those of YNCD4 T cell blasts (Fig. 5A). The frequency of cells upregulating CD69 at 6 or 24 h post-secondary activation was also comparable between the Yg and Ad groups (data not shown). We also estimated the frequencies of these cells undergoing death by annexin V and found no differences between ANCD4 and YNCD4 cells (Fig. 5B). These data suggest that cells in ANCD4 populations that do survive the first couple of divisions may generate progeny comparable to YNCD4 progeny in their susceptibility to death.

These data suggest that effector cells generated as a result of naive T cell activation *in vivo* in Ad animals could be functionally normal, at least with regard to their susceptibility to death. To test this, we sorted *ex vivo* purified EM cells and ANCD4 cells and YNCD4 cells and activated them with anti-CD3 and anti-CD28 *in vitro*. The EM cells from Ad mice, like ANCD4 cells, proliferated poorly in response to titrating doses of anti-CD3 (Fig. 5C). However, as in the case of T cell blasts generated *in vitro*, they were no more susceptible to death on activation than EM cells from Yg mice (Fig. 5D, left panel). Control ANCD4 cells, however, showed greater death on activation than YNCD4 cells as expected (Fig. 5D, right panel). These data suggest that the *in vivo* environment in Ad mice may differentially affect different functions in responding CD4 T cell populations.

Reduced efficiency of differentiation of ANCD4 cells to the CM phenotype in vitro

In order to test if the tendency of ANCD4 cells to die in response to primary activation led to relatively lower numbers of extensively proliferated cells, we examined the numbers of live (annexin V-negative) CFSE-labelled cells in activation cultures as above to estimate surviving cells in each successive generation. The results show that total viable cell yields from ANCD4 cultures were low and there were fewer Ad cells in every division as compared with Yg cells (Fig. 6A).

Among memory-phenotype ($CD44^{high}$) CD4 T cells, the $CD62L^{high}$ CM cells are reported to be the major population involved in proliferative recall responses (35,36). There is some evidence that extensively proliferated T cells are more likely to become CM cells (37), although this is not observed in all systems examined (38). In this context, we asked if ANCD4 cells would show relative paucity of CM phenotype cells in activation cultures. ANCD4 and YNCD4 cells were

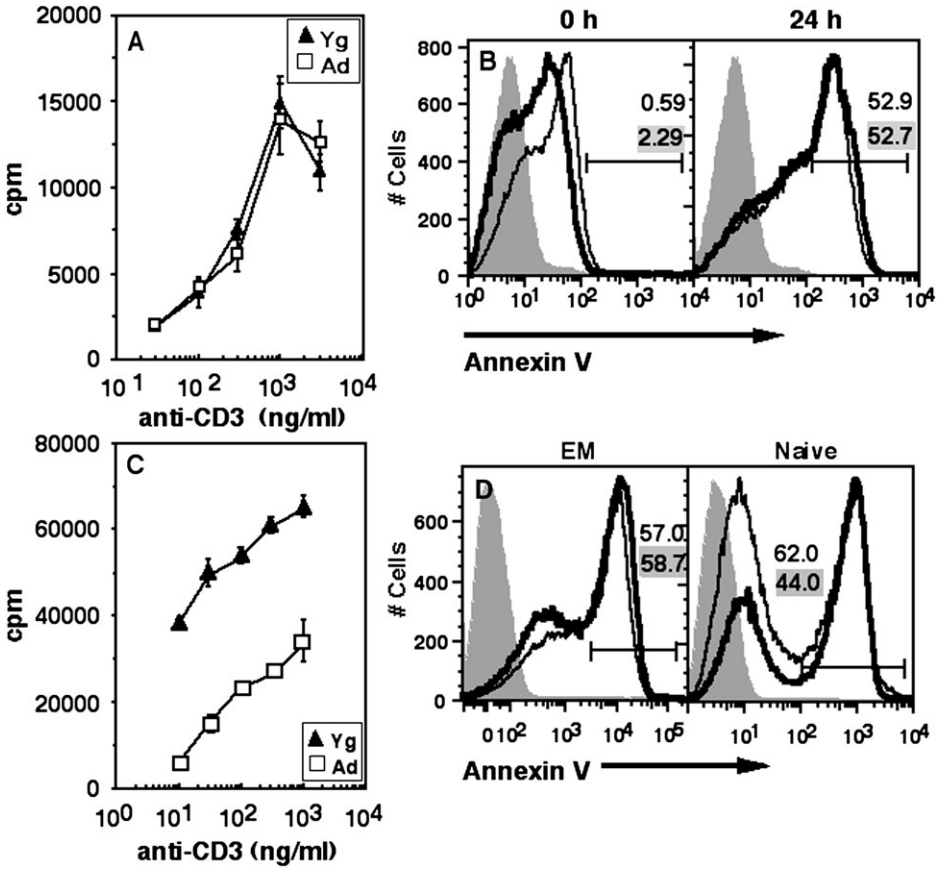

Fig. 5. Ad and Yg CD4 T cell blasts and EM cells *ex vivo* show comparable susceptibility to activation-induced death. (A) Ad and Yg CD4 T cell blasts recovered 96 h post-activation by Ficoll separation were re-stimulated with titrating doses of anti-CD3. Proliferation was measured by [^{3}H]thymidine incorporation (mean ± SEM of triplicate cultures). (B) Cells re-stimulated as in (A) above were scored at 0 and 24 h post-activation for annexin V staining. Shaded curve: negative control; thin line: Yg; thick line: Ad. Numbers in grey background are for Yg, and those in white background are for Ad. (C) Response of MACS-purified *ex vivo* EM cells from Yg and Ad mice to titrating doses of anti-CD3. Proliferation was measured by [^{3}H]thymidine incorporation (mean ± SEM of triplicate cultures). (D) MACS-purified EM (left) and naive (right) cells were activated for 48 h and death was scored by annexin V. Shaded curve: negative control; thin line: Yg; thick line: Ad.

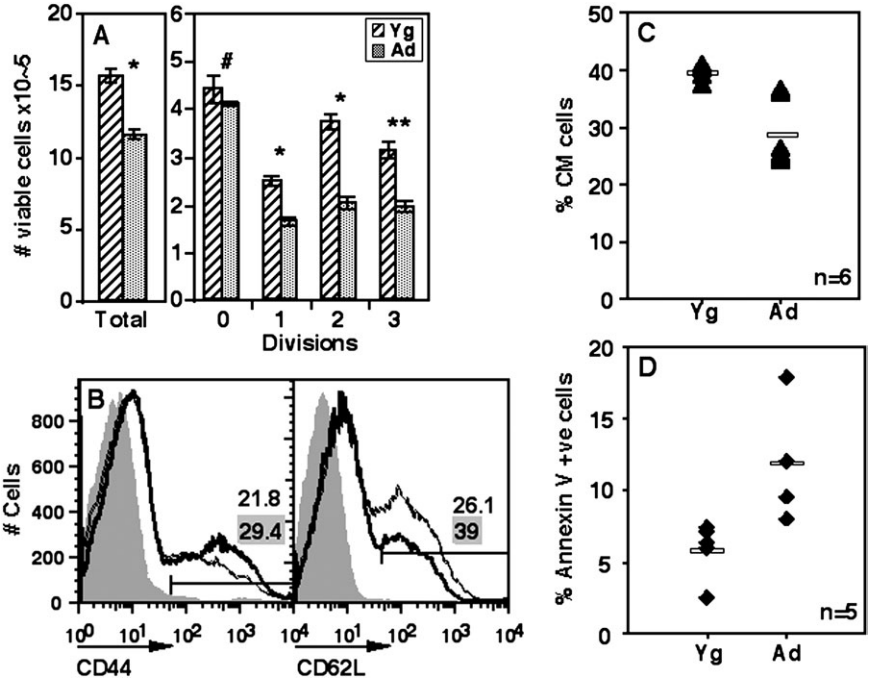

Fig. 6. ANCD4 cells show poor generation of the CM phenotype *in vitro*. (A) Total number of viable cells (left panel) and viable cells in each division from CFSE-labelled activated YNCD4 and ANCD4 cell cultures at 60 h (right panel). Mean ± SEM, $n = 3$. *$P < 0.005$, **$P < 0.01$, #$P > 0.05$. (B) CD44 staining in activated YNCD4 and ANCD4 cells at 48 h (left panel). CD44-positive cells gated as shown were stained for CD62L ($CD62L^{high}$, CM), right panel. Thin lines: YNCD4; thick lines: ANCD4. Numbers with grey background are for YNCD4; numbers with white background are for ANCD4. (C) Pooled data from multiple experiments as in (B) above showing CM cells as a percentage of $CD44^{high}$ cells from Yg and Ad mice. $P = 0.0026$ by Mann–Whitney test; n as indicated. Horizontal line depicts mean value. (D) Proportions of annexin V-positive cells in CM populations in experiments as in (B) above. $P = 0.006$ by Mann–Whitney test; n as indicated. Horizontal line depicts mean value.

stimulated *in vitro* and were stained at 48 h (and 60 h, data not shown) post-activation for CD44, CD62L and annexin V and CM ($CD44^{high}$ $CD62L^{high}$) cell frequencies among the $CD44^{high}$ cells were determined (Fig. 6B). Data from multiple experiments showed that the proportions of CM cells were significantly lower in ANCD4 than in YNCD4 cultures (Fig. 6C). Further, CM phenotype cells in the Ad group showed greater frequencies of apoptosis than the equivalent populations from the Yg group (Fig. 6D).

Relative reduction in CD4 T cells of the CM phenotype in vivo in Ad mice

A prediction from the *in vitro* data above was that Ad mice would have relatively fewer CM phenotype cells in their memory CD4 T cell compartment. We tested this prediction by examining the frequencies of CD4 T cells of the CM phenotype in the spleens of Yg and Ad mice. As expected, Ad mice showed a greater prominence of $CD44^{high}$ memory CD4 cells than Yg mice (Fig. 7A, left panel). Among $CD44^{high}$ cells, however, Ad mice showed a relative paucity of $CD62L^{high}$ CM phenotype cells (Fig. 7A, right panel), and analysis of data from multiple individual mice showed that Ad mice had significantly lower proportions of CM cells (Fig. 7B).

Ad T cells, as noted above, do show poor activation of Rel family transcription factors, particularly c-Rel which has been implicated in the survival of activated T cells *in vivo* (39). We therefore estimated the proportion of CM cells in Yg (8- to 10-week-old) c-Rel-null mice in comparison with C57BL/6 wild type (WT) mice. While c-Rel-null mice showed no difference from WT mice in the frequency of $CD44^{high}$ memory CD4 cells (data not shown) they showed lower proportions of CM cells (Fig. 7C, left panel). In order to check the role of Fas–FasL interaction in controlling the immune memory *in vivo*, we compared the proportions of CM cells in Yg B6.lpr mice with age-matched WT mice and found no difference (Fig. 7C, right panel).

The above data suggested that during the evolution of a T cell response to exogenous protein immunization, the magnitude of the response in Ad mice would be poorer than that in Yg mice and would get progressively worse. We tested this by immunizing Ad or Yg mice with a strong immunogen, mOA in CFA subcutaneously. Draining lymph node cells were harvested at 7, 28 or 45 days post-immunization and stimulated *in vitro* with mOA. IFN-gamma was assayed in the culture supernatants. Ad T cells produced lower levels of IFN-gamma early post-immunization and the response decayed rapidly over time as compared with Yg T cells (Fig. 7D).

Discussion

The data presented here refine our understanding of the poor responses of ANCD4 cells. We demonstrate that these cells have a poor ability to respond to metabolic demands, as well as increased susceptibility to DNA damage

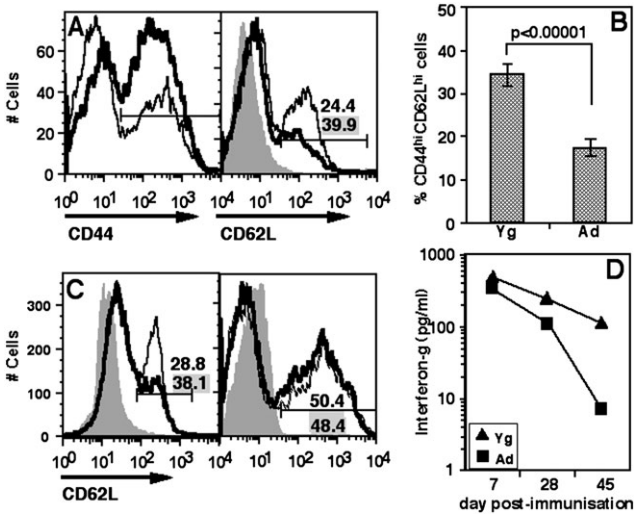

Fig. 7. Poor CM in CD4 cells in Ad mice. (A) CD4 cells were gated from stained splenic cell populations of individual mice (data not shown). CD44 gating on CD4 cells is shown (left panel). On gated CD44 cells, CD62L staining and CM gate is shown in the right panel. Thin lines: Yg mice; thick lines: Ad mice. Numbers with grey background are for Yg mice; numbers with white background are for Ad mice. (B) Pooled data as in (A) above from Yg and Ad mice showing CM cells as a proportion of $CD44^+$ cells in splenic CD4 cells. Mean ± SEM, $n = 17$. (C) A representative plot to show proportions of CM cells from WT and c-Rel-null (left panel) and WT and B6.lpr (right panel) mice in splenic CD4 cells. Gating for CD44 as in (A) above (data not shown). Thin line: WT mice; thick line: c-Rel-null (left) or B6.lpr (right) mice. Numbers with grey background are for WT mice; numbers with white background are for c-Rel-null (left) or B6.lpr (right) mice. (D) IFN-gamma levels in culture supernatants from mOA recall assays *in vitro* on lymph node cells from Yg and Ad mice immunized with mOA 7, 28 and 45 days prior to assay.

controlling survival during primary activation. We also identify a functionally significant correlate of the poor survival of proliferating CD4 T cells during primary responses, namely, a reduction in the ability to generate CM CD4 T cells.

T cells from the aged mice are considered to be defective and there are many facets to these defects. The behavioural differences in naive and memory T cells from the Ad have been examined, by and large, using TCR-transgenic mouse strains. While these monoclonal transgenic TCR systems provide definitive identification of naive and memory T cells, they also make analogous analyses in non-manipulated systems essential. We have focussed our study on CD4 T cells.

We report a distinct difference between the susceptibility of ANCD4 and YNCD4 cells to death in response to primary activation. This death pathway appears to originate in mitochondria, results in subdiploid DNA and is seen in cells that have successfully responded to some extent to activation, since CD69-expressing cells in the ANCD4 population also show more death than equivalent YNCD4 cells do.

Many mitochondrial defects are associated with ageing (40–42). Mitochondria are also crucially involved in autophagy and cell survival (43). We show here that within the first 12 h of activation, many more ANCD4 T cells show an early loss of mitochondrial membrane potential before they die, suggesting a role of mitochondrial pathways in this apoptotic decision.

Classical activation-induced cell death in T cells follows the extrinsic pathway of cell death, is dependent on Fas–FasL interactions (44) and has been attributed as one of the causes for T cell deficiency in Ad human beings (45). Our data on naive CD4 T cells from Yg CD95 (Fas)-deficient B6.lpr mice showed frequencies of death early during primary activation similar to C57BL/6-wild-type (B6.WT) mice (data not shown), suggesting that this cell death decision does not involve CD95–CD95L interactions. Comparable proportions of CM cells *ex vivo* between B6.lpr and B6.WT mice also support this notion.

We observe that unstimulated resting ANCD4 cells survive better than YNCD4 cells, indicating that ANCD4 cells are not globally more susceptible to intrinsic apoptosis, but become specifically more susceptible to mitochondrial death upon activation. Activation of T cells enhances their metabolic requirements, and activated T cells upregulate anaerobic glycolysis to generate pyruvate and lactate (46). Thus, poor lactate production may be indicative of the failure of ANCD4 cells to upregulate glycolysis in response to activation. In turn, poor lactate production may contribute to poor cellular anabolic responses (46) and may thus be a factor in compromised survival during primary activation.

A major pathway for meeting enhanced metabolic demands is the induction of autophagy (47). Autophagy plays multiple roles in organismal survival and homoeostasis and one of the functions it serves is that of self-digestion induced by nutrient deprivation or increased metabolic demand (47,48). Autophagic vacuoles are marked by a localization of LC3 (49). ANCD4 cells appear to be poor in activation-induced autophagy compared with YNCD4 cells. Use of monodansyl cadaverine as a marker of autophagic cells also supports these findings (data not shown). The observation that an inhibitor of autophagy enhances the low levels of early death seen in activated YNCD4 cells indicates that the autophagy seen in activated YNCD4 cells contributes to survival and that its absence in ANCD4 cells may be a factor in their enhanced apoptosis.

Naive T cells responding to primary activation rapidly enter cell cycle. DNA replication during cell cycle is associated with potential DNA breaks (50), and DNA break repair mechanisms are critical to the ability of cells to pass cell cycle checkpoints (51). It is known that with organismal ageing the ability of cells to sense and repair DNA decreases (52). Our data demonstrate that activated ANCD4 cells show significantly increased occurrence of DNA damage after activation as well as upon gamma-irradiation.

We also found that susceptibility of ANCD4 cells to apoptotic death on activation persisted through the first couple of generations of cell division. Cell cycle analysis 40 h post-activation showed higher proportions of subdiploid apoptotic cells and fewer cells in S/G2/M stages in ANCD4 population (data not shown). When CD44 was used as a late activation marker, cells which were successfully upregulating CD44 (and were expected to be progressing through cell division) also showed greater frequency of apoptosis. During early generations as identified by CFSE dilution the proportion of dying cells tended to be higher in the Ad group, indicating

that ANCD4 cells remained more susceptible to death at least through the first couple of cell cycles in response to primary activation. Thus, the enhanced death of Ad T cells upon activation is not simply an alternative to non-entry into cell cycle, since it is seen even in Ad T cells that have successfully gone through one cell division. However, whether there is a separate defect in cell-cycle entry or not remains unclear.

The quantitatively higher death susceptibility of activated ANCD4 cells during initial divisions does not appear to persist after further divisions over time. Thus, those ANCD4 cells that survive the first couple of divisions *in vitro* upon activation are not different from their YNCD4 counterparts in terms of death susceptibility. In fact, their ability to proliferate upon being re-stimulated is also no different from that of their Yg counterparts. These data suggest that rather than ageing at the cellular level being associated with the time elapsed since a daughter cell was born, T cell populations from Ad mice undergoing activation *in vitro* may show either progressive dilution of epigenetic factors enhancing commitment to cell death over successive divisions or that such activated Ad T cells are subjected to selection events where they show enhanced susceptibility to cell death early during proliferation, but eventually populations that survive to enter later rounds of proliferation do not show this death phenotype.

The prediction of these findings is that those effector cells that are generated as a result of naive T cell activation *in vivo* in Ad animals should be functionally normal. Our data demonstrate that EM cells from Ad mice show poor proliferative responses to activation *in vitro*, in contrast to recently activated ANCD4 cells. However, these *ex vivo* EM CD4 cells do not show the enhanced death phenotype upon activation as ANCD4 cells do. Thus, a model emerges in which naive Ad CD4 T cells, upon activation, tend to die more during early stages of activation, with the result that a population that does not show this property emerges during later rounds of proliferation. This population is initially normal as far as proliferative and death responses to activation are concerned, but eventually they re-acquire one defect, that in proliferation (and perhaps in cytokine secretion), but not the other defect, namely enhanced death. This may be the consequence of residual epigenetic alterations and/or poor microenvironmental signalling *in vivo*. Using TCR-transgenic T cells it has been suggested that the age of the naive T cell *per se* and not the age of the organism accounts for the poor T cell response (53) and our data from non-transgenic mice imply that the age of individual naive T cells and the environment they face together might contribute to the complex phenotype observed.

As naive T cells go through successive cell divisions in response to antigenic stimulation, they also undergo differentiation. Some previous reports have shown that initial differentiation concomitant with early rounds of division results in generation of EM cells which proliferate poorly but make cytokines rapidly upon re-stimulation, and that maturation to the CM phenotype occurs in cells that have undergone multiple rounds of division (36). While this association of extensive proliferation and CM differentiation has not been observed in all instances (38), it is notable that, due in part to early and continuing death during primary activation, ANCD4 cell cultures had lower proportions of extensively proliferated cells as well as fewer cells showing the CM phenotype. While addition of IL-2 brought some improvement in CM differentiation (data not shown), the defect in Ad T cells was not fully compensated, suggesting that both IL-2-dependent and IL-2-independent factors could be involved. Lending further support to this, we found poor CM frequencies in the peripheral lymphoid organs of Ad mice *in vivo*. Based on the poor nuclear translocation of NF-κB family members p65 and c-Rel in Ad T cells, we predicted and demonstrated poor proportions of CM cells in T cells from Yg c-Rel-null mice as well.

A poor efficiency of CM commitment in ANCD4 cells suggests that the CD4 T cell response to immunization would decay more rapidly in Ad mice than in Yg mice. Indeed, in response to immunization, IFN-gamma-producing potential of Ad T cells, which was poor to begin with at day 7 post-immunization, dropped rapidly by day 45.

Thus, our data document a role for an early death pathway, possibly related to the lack of adequate responses to metabolic and cell cycle demands, in limiting the naive CD4 T cell response to activation in Ad mice, contributing to a reduction in the efficiency of generation of stable CM.

Supplementary data

Supplementary data are available at *International Immunology* Online.

Funding

Indo-US Vaccine Action Plan (to A.G., V.B., S.R. and J.M.D.); the Department of Biotechnology and the Department of Science and Technology, Government of India (to A.G., S.R. and V.B.); the National Institutes of Health, USA (1R15AG017472-01, 1R03AI070312-01A2 and 3R15AG017472-01S1 to J.M.D.); and the Arkansas Biotechnology Institute (to J.M.D.).

Acknowledgements

We thank H. C. Liou (Cornell University, New York, NY, USA) and Ranjan Sen (National Institute on Ageing, NIH, Bethesda, MD, USA) for the gift of c-Rel-null mice. We thank R. K. Juyal, Small Animal Facility, National Institute of Immunology, for the breeding and supply of mice. The National Institute of Immunology is supported by the Department of Biotechnology, Government of India.

Abbreviations

3-MA	3-methyl adenine
ANCD4 cells	naive CD4 cells from aged mice
Ad	aged
aged T cells	T cells from aged mice
CFSE	carboxyfluorescein succinimidyl ester
CM	central memory
$DiOC_6$	3,3′-dihexyloxacarbocyanine iodide
EM	effector memory
LC3	microtubule-associated protein light chain-3
mOA	maleylated ovalbumin
NIH	National Institutes of Health
PI	propidium iodide
WT	wild type
YNCD4 cells	naive CD4 cells from young mice
Yg	young

References

1 Linton, P. and Thoman, M. L. 2001. T cell senescence. *Front. Biosci.* 6:D248.
2 Miller, R. A. 1996. The aging immune system: primer and prospectus. *Science* 273:70.
3 Pawelec, G., Solana, R., Remarque, E. and Mariani, E. 1998. Impact of aging on innate immunity. *J. Leukoc. Biol.* 64:703.
4 Ginaldi, L., De Martinis, M., D'Ostilio, A. *et al.* 1999. The immune system in the elderly: I. Specific humoral immunity. *Immunol. Res.* 20:101.
5 Haynes, L., Linton, P. J. and Swain, S. L. 1997. Age-related changes in CD4 T cells of T cell receptor transgenic mice. *Mech. Ageing Dev.* 93:95.
6 McElhaney, J. E., Meneilly, G. S., Beattie, B. L. *et al.* 1992. The effect of influenza vaccination on IL2 production in healthy elderly: implications for current vaccination practices. *J. Gerontol.* 47:M3.
7 Haynes, L., Linton, P. J., Eaton, S. M., Tonkonogy, S. L. and Swain, S. L. 1999. Interleukin 2, but not other common gamma chain-binding cytokines, can reverse the defect in generation of CD4 effector T cells from naive T cells of aged mice. *J. Exp. Med.* 190:1013.
8 Hale, J. S., Boursalian, T. E., Turk, G. L. and Fink, P. J. 2006. Thymic output in aged mice. *Proc. Natl Acad. Sci. USA* 103:8447.
9 Clise-Dwyer, K., Huston, G. E., Buck, A. L., Duso, D. K. and Swain, S. L. 2007. Environmental and intrinsic factors lead to antigen unresponsiveness in CD4(+) recent thymic emigrants from aged mice. *J. Immunol.* 178:1321.
10 Agrawal, A., Agrawal, S. and Gupta, S. 2007. Dendritic cells in human aging. *Exp. Gerontol.* 42:421.
11 Aspinall, R. 2006. T cell development, ageing and interleukin-7. *Mech. Ageing Dev.* 127:572.
12 Ortiz-Suarez, A. and Miller, R. A. 2003. Antigen-independent expansion of CD28hi CD8 cells from aged mice: cytokine requirements and signal transduction pathways. *J. Gerontol. A Biol. Sci. Med. Sci.* 58:B1063.
13 Marko, M. G., Ahmed, T., Bunnell, S. C. *et al.* 2007. Age-associated decline in effective immune synapse formation of CD4(+) T cells is reversed by vitamin E supplementation. *J. Immunol.* 178:1443.
14 Haynes, L., Eaton, S. M. and Swain, S. L. 2000. The defects in effector generation associated with aging can be reversed by addition of IL-2 but not other related gamma(c)-receptor binding cytokines. *Vaccine* 18:1649.
15 Eisenbraun, M. D., Tamir, A. and Miller, R. A. 2000. Altered composition of the immunological synapse in an anergic, age-dependent memory T cell subset. *J. Immunol.* 164:6105.
16 Hsu, H. C., Shi, J., Yang, P. *et al.* 2001. Activated CD8(+) T cells from aged mice exhibit decreased activation-induced cell death. *Mech. Ageing Dev.* 122:1663.
17 Gupta, S. and Gollapudi, S. 2006. Molecular mechanisms of TNF-alpha-induced apoptosis in naive and memory T cell subsets. *Autoimmun. Rev.* 5:264.
18 Gupta, S. and Gollapudi, S. 2008. CD95-mediated apoptosis in naive, central and effector memory subsets of CD4+ and CD8+ T cells in aged humans. *Exp. Gerontol.* 43:266.
19 Zhang, X., Fujii, H., Kishimoto, H., LeRoy, E., Surh, C. D. and Sprent, J. 2002. Aging leads to disturbed homeostasis of memory phenotype CD8(+) cells. *J. Exp. Med.* 195:283.
20 Van Remmen, H. and Richardson, A. 2001. Oxidative damage to mitochondria and aging. *Exp. Gerontol.* 36:957.
21 Monti, D., Salvioli, S., Capri, M. *et al.* 2000. Decreased susceptibility to oxidative stress-induced apoptosis of peripheral blood mononuclear cells from healthy elderly and centenarians. *Mech. Ageing Dev.* 121:239.
22 Eaton, S. M., Burns, E. M., Kusser, K., Randall, T. D. and Haynes, L. 2004. Age-related defects in CD4 T cell cognate helper function lead to reductions in humoral responses. *J. Exp. Med.* 200:1613.
23 Coleman, C., Howell, K., Hobbs, M. V. and Riggs, J. E. 2006. Age-dependent loss of naive T cells in TCR transgenic bone marrow chimeras. *Immunobiology* 211:701.
24 Abraham, R., Singh, N., Mukhopadhyay, A., Basu, S. K., Bal, V. and Rath, S. 1995. Modulation of immunogenicity and antigenicity of proteins by maleylation to target scavenger receptors on macrophages. *J. Immunol.* 154:1.
25 Vig, M., Srivastava, S., Kandpal, U. *et al.* 2004. Inducible nitric oxide synthase in T cells regulates T cell death and immune memory. *J. Clin. Invest.* 113:1734.
26 Olive, P. L. and Banath, J. P. 2006. The comet assay: a method to measure DNA damage in individual cells. *Nat. Protoc.* 1:23.
27 Frauwirth, K. A., Riley, J. L., Harris, M. H. *et al.* 2002. The CD28 signaling pathway regulates glucose metabolism. *Immunity* 16:769.
28 Annett, K., Hyland, P., Duggan, O., Barnett, C. and Barnett, Y. 2004. An investigation of DNA excision repair capacity in human CD4+ T cell clones as a function of age in vitro. *Exp. Gerontol.* 39:491.
29 Ferreira, V., Sidenius, N., Tarantino, N. *et al.* 1999. *In vivo* inhibition of NF-kappa B in T-lineage cells leads to a dramatic decrease in cell proliferation and cytokine production and to increased cell apoptosis in response to mitogenic stimuli, but not to abnormal thymopoiesis. *J. Immunol.* 162:6442.
30 Trebilcock, G. U. and Ponnappan, U. 1996. Induction and regulation of NFkappaB during aging: role of protein kinases. *Clin. Immunol. Immunopathol.* 79:87.
31 Trebilcock, G. U. and Ponnappan, U. 1996. Evidence for lowered induction of nuclear factor kappa B in activated human T lymphocytes during aging. *Gerontology* 42:137.
32 Mittal, A., Papa, S., Franzoso, G. and Sen, R. 2006. NF-kappaB-dependent regulation of the timing of activation-induced cell death of T lymphocytes. *J. Immunol.* 176:2183.
33 Venkataraman, L., Burakoff, S. J. and Sen, R. 1995. FK506 inhibits antigen receptor-mediated induction of c-rel in B and T lymphoid cells. *J. Exp. Med.* 181:1091.
34 Mizushima, N., Levine, B., Cuervo, A. M. and Klionsky, D. J. 2008. Autophagy fights disease through cellular self-digestion. *Nature* 451:1069.
35 Bachmann, M. F., Wolint, P., Schwarz, K. and Oxenius, A. 2005. Recall proliferation potential of memory CD8+ T cells and antiviral protection. *J. Immunol.* 175:4677.
36 Bouneaud, C., Garcia, Z., Kourilsky, P. and Pannetier, C. 2005. Lineage relationships, homeostasis, and recall capacities of central- and effector-memory CD8 T cells in vivo. *J. Exp. Med.* 201:579.
37 Opferman, J. T., Ober, B. T. and Ashton-Rickardt, P. G. 1999. Linear differentiation of cytotoxic effectors into memory T lymphocytes. *Science* 283:1745.
38 Laouar, A., Manocha, M., Haridas, V. and Manjunath, N. 2008. Concurrent generation of effector and central memory CD8 T cells during vaccinia virus infection. *PLoS One* 3:e4089.
39 Saibil, S. D., Jones, R. G., Deenick, E. K. *et al.* 2007. CD4+ and CD8+ T cell survival is regulated differentially by protein kinase Ctheta, c-Rel, and protein kinase B. *J. Immunol.* 178:2932.
40 Singh, K. K. 2006. Mitochondria damage checkpoint, aging, and cancer. *Ann. NY Acad. Sci.* 1067:182.
41 Trifunovic, A. and Larsson, N. G. 2008. Mitochondrial dysfunction as a cause of ageing. *J. Intern. Med.* 263:167.
42 Navarro, A. and Boveris, A. 2007. The mitochondrial energy transduction system and the aging process. *Am. J. Physiol. Cell. Physiol.* 292:C670.
43 Pollack, M. and Leeuwenburgh, C. 2001. Apoptosis and aging: role of the mitochondria. *J. Gerontol. A Biol. Sci. Med. Sci.* 56:B475.
44 Mateo, V., Menager, M., de Saint-Basile, G. *et al.* 007. Perforin-dependent apoptosis functionally compensates Fas deficiency in activation-induced cell death of human T lymphocytes. *Blood* 110:4285.
45 Aggarwal, S. and Gupta, S. 1999. Increased activity of caspase 3 and caspase 8 in anti-Fas-induced apoptosis in lymphocytes from ageing humans. *Clin. Exp. Immunol.* 117:285.
46 Frauwirth, K. A. and Thompson, C. B. 2004. Regulation of T lymphocyte metabolism. *J. Immunol.* 172:4661.
47 Levine, B. and Kroemer, G. 2008. Autophagy in the pathogenesis of disease. *Cell* 132:27.
48 Cavallini, G., Donati, A., Taddei, M. and Bergamini, E. 2007. Evidence for selective mitochondrial autophagy and failure in aging. *Autophagy* 3:26.

49 Wang, Y., Han, R., Liang, Z. Q. *et al.* 2008. An autophagic mechanism is involved in apoptotic death of rat striatal neurons induced by the non-N-methyl-D-aspartate receptor agonist kainic acid. *Autophagy* 4:214.
50 Chowdhury, D., Xu, X., Zhong, X. *et al.* 2008. A PP4-phosphatase complex dephosphorylates gamma-H2AX generated during DNA replication. *Mol. Cell* 31:33.
51 Delacote, F. and Lopez, B. S. 2008. Importance of the cell cycle phase for the choice of the appropriate DSB repair pathway, for genome stability maintenance: the trans-S double-strand break repair model. *Cell Cycle* 7:33.
52 Sedelnikova, O. A., Horikawa, I., Redon, C. *et al.* 2008. Delayed kinetics of DNA double-strand break processing in normal and pathological aging. *Aging Cell* 7:89.
53 Haynes, L., Eaton, S. M., Burns, E. M., Randall, T. D. and Swain, S. L. 2005. Newly generated CD4 T cells in aged animals do not exhibit age-related defects in response to antigen. *J. Exp. Med.* 201:845.